International Journal of Heat and Mass Transfer 183 (2022) 122180

Contents lists available at ScienceDirect

International Journal of Heat and Mass Transfer

journal homepage: www.elsevier.com/locate/hmt

Analytical modeling of conjugate heat transfer between a bed of phase change material and laminar convective flow

Amirhossein Mostafavi, Ankur Jain*

Mechanical and Aerospace Engineering Department, University of Texas at Arlington, Arlington, TX, USA

ARTICLE INFO

Article history:
Received 13 September 2021
Revised 17 October 2021
Accepted 24 October 2021

Keywords:
Phase change energy storage
Convective heat transfer
Conjugate heat transfer
Perturbation method
Karman-Pohlhausen Polynomials

ABSTRACT

Latent heat of a phase change material (PCM) is commonly used for energy storage and thermal management. A flat bed configuration is commonly used in latent energy storage systems, in which, fluid flow over a PCM bed results in heat transfer to/from and melting/solidification of the PCM. Understanding the nature of heat transfer in such systems is critical for design and performance optimization. This paper presents an analytical model for conjugate heat transfer in a flat bed latent energy storage system. The model solves the governing energy conservation equations by utilizing the interfacial conditions to iterate between the PCM and fluid flow. Good convergence of the iterative technique is demonstrated. The model is used to study phase change propagation and energy storage as functions of various problem parameters such as imposed temperature difference, flow velocity and thermal properties of PCM and fluid flow. It is found that the convective heat transfer coefficient between the PCM and fluid flow is not constant, but, rather, is a function of space and time, and is affected by flow speed and properties, as well as thermal properties of the PCM. The general methodology presented here can be adapted for annular and other latent energy storage configurations. This work contributes towards a fundamental understanding of heat transfer processes in an important energy storage system that is commonly encountered in practical applications.

1. Introduction

Phase change materials (PCMs) are used commonly for latent energy storage [1] and thermal management [2]. For example, excess thermal energy produced in a Concentrated Solar Power (CSP) plant is often stored in the form of latent heat to be utilized when direct solar energy is not available [1]. Phase change heat transfer has also been investigated for transient thermal management of engineering systems such as electronics [2] and Li-ion cells [3].

Understanding the nature of heat transfer during latent energy storage in a PCM is critical for improving the efficiency of latent energy storage. This involves heat transfer both within the PCM and between the PCM and the heat source/sink. A significant amount of experimental investigation has been reported on heat transfer enhancement in latent energy storage systems by mechanisms such as improving thermal conductivity of the PCM [4], or providing fins within the PCM [5–7]. A number of analytical and numerical techniques have also been developed to model and optimize phase change processes, particularly the interaction between the PCM and the source/sink to/from where heat transfer occurs. On one hand, fundamental heat transfer modeling of the phase change process under various boundary conditions has been carried out. For example, perturbation method based solutions of phase change problems under time-dependent temperature [8] and heat flux [9] boundary conditions have been developed. Analytical and numerical models for the impact of fins on the rate of latent energy storage have been developed [5], and an optimal fin size has been demonstrated [6]. The impact of thermal properties such as thermal conductivity and heat capacity has also been investigated [10]. Most of these papers that analyze heat transfer only in the PCM represent the external heat source/sink in the form of an appropriate boundary condition. On the other hand, substantial literature also exists on theoretical and numerical modeling of practical latent heat energy storage geometries. For example, the problem of heat exchange between PCM and a fluid in cylindrical geometry has been analyzed [11–13]. Semi-analytical models have been proposed for flat plate latent heat storage, in which convective heat transfer between a flat bed of PCM and fluid flow over the bed is responsible for latent heat storage [14–16]. Numerical modeling has been used to analyze the impact of fins in a tubular latent heat energy storage unit [17]. Numerical modeling of phase change energy storage in spherical PCMs has also been presented [18].

* Corresponding author.
E-mail address: jaina@uta.edu (A. Jain).

https://doi.org/10.1016/j.ijheatmasstransfer.2021.122180
0017-9310/

Nomenclature

c	specific heat capacity, $Jkg^{-1}K^{-1}$
G	nondimensional heat flux, $G = \frac{q_s L}{k_p(T_\infty - T_m)}$
k	thermal conductivity, $Wm^{-1}K^{-1}$
$\bar{k}_f$	nondimensional fluid flow thermal conductivity, $k_f = \frac{k_f}{k_p}$
L	reference length scale, m
L_p	latent heat of fusion, Jkg^{-1}
Nu	Nusselt number
Pr	Prandtl number
q	heat flux, Wm^{-2}
$\bar{Q}$	nondimensional heat stored in the PCM, $\bar{Q} = \int_0^\tau \int_0^{\bar{W}} G \, d\xi \, d\tau$
Ste	Stefan number, $Ste = \frac{c_p(T_\infty - T_m)}{L_p}$
t	time, s
T	temperature, K
T_m	melting temperature, K
u,v	velocities in x and y directions, ms^{-1}
$\bar{u},\bar{v}$	nondimensional velocities in ξ and η directions respectively, $\bar{u} = \frac{uL}{\alpha_p}$, $\bar{v} = \frac{vL}{\alpha_p}$
U_∞	freestream velocity, ms^{-1}
$\bar{U}_\infty$	nondimensional freestream velocity, $\bar{U}_\infty = \frac{U_\infty L}{\alpha_p}$
W	length of the PCM bed, m
$\bar{W}$	nondimensional length of the PCM bed, $\bar{W} = \frac{W}{L}$
x, y	spatial coordinates, m

Greek symbols

α	thermal diffusivity, m^2s^{-1}
$\bar{\alpha}_f$	nondimensional fluid flow thermal diffusivity, $\bar{\alpha}_f = \frac{\alpha_f}{\alpha_p}$
δ	boundary layer thickness, m
$\bar{\delta}$	nondimensional boundary layer thickness, $\bar{\delta} = \frac{\delta}{L}$
ξ, η	nondimensional spatial coordinates, $\xi = \frac{x}{L}$, $\eta = \frac{y}{L}$
θ_f	nondimensional fluid flow temperature, $\theta_f = \frac{T_\infty - T_f}{T_\infty - T_m}$
θ_p	nondimensional PCM temperature, $\theta_p = \frac{T_p - T_m}{T_\infty - T_m}$
θ_s	nondimensional interface temperature, $\theta_s = \frac{T_\infty - T_s}{T_\infty - T_m}$
ν	kinematic viscosity, m^2s^{-1}
ρ	mass density, kgm^{-3}
τ	nondimensional time, $\tau = \frac{\alpha_p t}{L^2}$

Subscripts

f	fluid flow
LS	solid-liquid interface
p	phase change material
s	PCM- fluid flow interface
t	thermal
∞	freestream

Amongst the various geometries for a latent heat energy storage system outlined above, the flat bed geometry is one of the simplest and most commonly used. As shown schematically in Fig. 1, in this geometry, convective heat transfer due to fluid flow over one or more flat PCM beds, usually arranged in parallel is responsible for phase change and latent heat storage. Despite its geometrical simplicity, heat transfer modeling of a flat bed PCM is not straight-forward. On one hand, phase change in the bed is, in general, non-linear in nature [19]. On the other hand, fluid flow and convective heat transfer over the bed is also, in general, non-linear [20]. In general, the convective heat transfer coefficient between the bed and fluid flow is a function of both space and time, and is not known in advance because neither the temperature nor the heat flux at the PCM-fluid interface is known. While a few papers have attempted to develop an analytical heat transfer model for a flat bed phase change system [15,16], these papers assumed values/expressions for the convective heat transfer coefficient corresponding to isothermal and constant flux boundary conditions, which is clearly not valid for the PCM-flow interface due to dynamic boundary layer growth and phase change front propagation. In a general problem, the convective heat transfer coefficient must be determined by solving the underlying equations, and can not be assumed in advance.

In order to overcome these shortcomings, it is important to treat the PCM-fluid heat transfer problem as a conjugate problem. Conjugate heat transfer problems involve more than one significant modes of heat transfer [21], most commonly convective heat transfer in a fluid flow and conduction heat transfer in a solid. In addition to these modes, the present problem is further complicated by the occurrence of phase change in the PCM. A conjugate phase change heat transfer analysis is expected to result in the phase change front as a function of time and convective heat transfer coefficient at the interface as a function of space and time.

An iterative technique has been proposed in the recent past to solve conjugate heat transfer problems [22]. This technique assumes a temperature distribution at the interface between the two regions in the problem, and solves the heat transfer problem in one of the regions by using the temperature distribution as a boundary condition for that region. The resulting interfacial heat flux distribution is used to solve the heat transfer problem in the other region, which is then used to update the interfacial temperature distribution. A few iterations of this process have been shown to result in a converged temperature distribution. This technique has been used for solving steady-state [22,23] and transient problems [24], including those with phase change heat transfer [24], as well as mass transfer problems [25].

This paper presents iterative analytical modeling of a flat bed latent energy storage system, in which phase change is driven by convective flow past the PCM bed. This work overcomes the shortcomings of past attempts at solving this problem by deriving a closed-form solution without assuming an expression for the convective heat transfer coefficient between the PCM bed and fluid flow. An iterative technique is used to solve the phase change and convective heat transfer problems. While the phase change problem is solved using a perturbation method, the convective heat transfer problem is solved by representing the flow velocity and temperature distributions using Karman-Pohlhausen polynomials [20,26]. Convergence of the temperature distribution over multiple iterations is demonstrated, and is used to predict the evolution of the phase change front in the PCM over time. Good agreement with finite-element simulations is demonstrated. The resulting analytical model is used to understand the impact of various problem parameters on the performance of latent heat energy storage.

2. Mathematical Modeling

2.1. Problem Definition

Fig. 1(a) shows a schematic of a flat bed latent heat storage system, in which a fluid flows over multiple parallel PCM beds and convective heat transfer between the two results in phase change energy storage driven by melting or solidification of the PCM bed. Due to symmetry in the geometry, a representative unit cell highlighted in Fig. 1(a) and shown in detail in Fig. 1(b) may be considered for analysis. A number of assumptions are made to facilitate analysis of this problem. On the fluid side, steady laminar flow

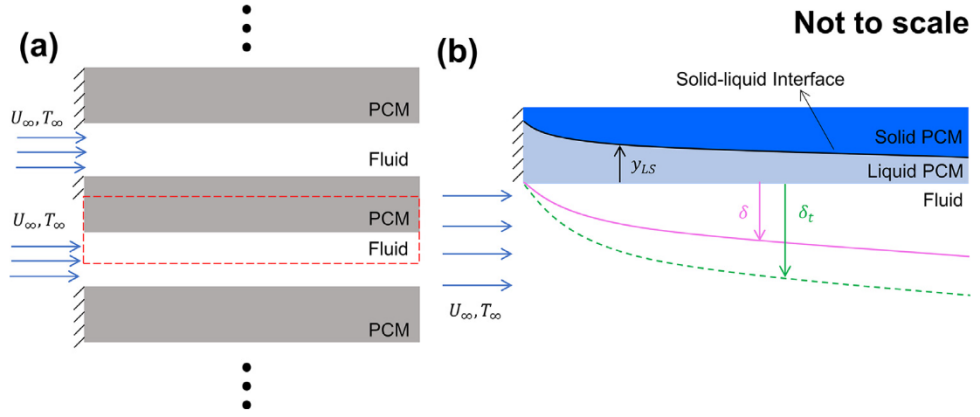

Fig. 1. (a) Schematic of a flat bed storage system comprising several flat PCM beds in parallel and convective heat transfer to/from a fluid flow, also showing a symmetry unit cell; (b) schematic of a single PCM-flow system in a symmetry unit cell. Schematics are not to scale.

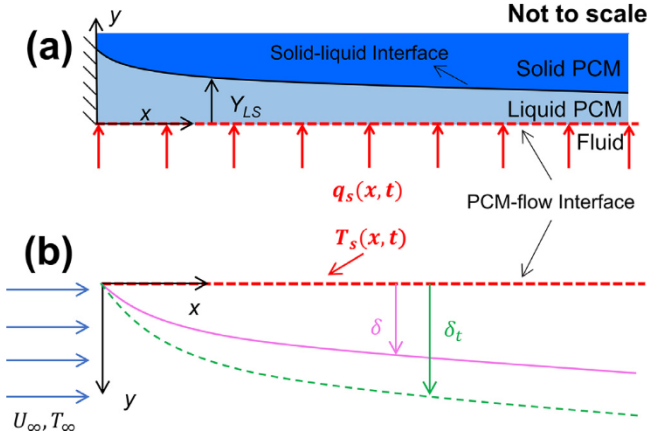

Fig. 2. Schematics of the (a) PCM and (b) flow sub-problems within the main problem, that are discussed in sections 2.2 and 2.3, respectively. These schematics show the geometry, coordinate system, boundary layers and phase change front. Interfacial heat flux and temperature at the interface between the sub-problems are also shown. Schematics are not to scale.

is assumed, with a uniform freestream velocity U_∞ and temperature T_∞. All properties are assumed to be independent of temperature. Due to constant viscosity, changes in temperature field over time do not influence the steady flow field. Viscous dissipation is assumed to be negligible. On the PCM side, heat flow and phase change are assumed to be one-dimensional, i.e., there is no heat transfer within the PCM in the x direction (please refer to Fig. 2(a) for coordinate direction), so that temperature distribution and location of the phase change front at any x in the PCM is assumed to be influenced only by the interface condition at that x, and not by the interface condition at other locations. Similar to the fluid, PCM thermal properties are also assumed to be independent of temperature. The PCM is assumed to be initially in solid phase at the melting temperature T_m. Convection in the liquid phase is neglected. Finally, it is also assumed that the fluid flow and PCM are separated by a thin plate of negligible thermal resistance and capacitance. The case of $T_\infty > T_m$ is considered here, leading to heat flow into the PCM and propagation of the melting front into the PCM over time. The opposite case of freezing of liquid PCM by flow of a cold fluid can also be analyzed using the techniques discussed here.

Based on the assumptions listed above, and referring to the coordinate system shown in Fig. 2(b), the momentum and energy conservation equations governing the velocity and temperature fields in the fluid flow are given by

$$\frac{\partial u}{\partial x} + \frac{\partial v}{\partial y} = 0 \tag{1}$$

$$u\frac{\partial u}{\partial x} + v\frac{\partial u}{\partial y} = \nu_f \frac{\partial^2 u}{\partial y^2} \tag{2}$$

$$\alpha_f \frac{\partial^2 T_f}{\partial y^2} = \frac{\partial T_f}{\partial t} + u\frac{\partial T_f}{\partial x} + v\frac{\partial T_f}{\partial y} \tag{3}$$

The associated boundary conditions are

$$u = U_\infty;\ T_f = T_\infty \qquad \text{at x} = 0 \tag{4}$$

$$u = 0; v = 0 \qquad \text{at y} = 0 \tag{5}$$

$$u = U_\infty \qquad \text{at y} \geq \delta \tag{6}$$

$$T_f = T_\infty \qquad \text{at y} \geq \delta_t \tag{7}$$

Where δ and δ_t refer to hydrodynamic and thermal boundary layer thicknesses, respectively.

Referring to the coordinate system shown in Fig. 2(a), the governing energy conservation equation on the PCM side is given by

$$\alpha_p \frac{\partial^2 T_p}{\partial y^2} = \frac{\partial T_p}{\partial t} \tag{8}$$

with

$$T_p = T_m \qquad \text{at y} = \text{y}_{LS} \tag{9}$$

Energy balance at the phase change interface yields the following equation for the evolution of the phase change front location with time

$$\rho_p L_p \frac{dy_{LS}}{dt} = -k_p \frac{\partial T_p}{\partial y} \qquad \text{at y} = \text{y}_{LS} \tag{10}$$

PCM and fluid temperature fields are assumed to be initially at the PCM melting temperature and freestream temperature respectively, i.e. $T_p = T_m$ and $T_f = T_\infty$ at t=0.

In addition to the equations above, temperature and heat flux conservation apply at the interface. As a result, one may write

$$T_f = T_p = T_s(x,t) \qquad \text{at y} = 0 \tag{11}$$

and

$$k_f \frac{\partial T_f}{\partial y} = -k_p \frac{\partial T_p}{\partial y} = q_s(x,t) \qquad \text{at y} = 0 \tag{12}$$

where $T_s(x,t)$ and $q_s(x,t)$ are the temperature and heat flux into the PCM at the PCM-flow interface. Note that the y coordinate in the first two terms in Eq. (12) corresponding to the flow and PCM problems, respectively, are in opposite directions, as shown in Figs. 2(a) and 2(b). T_s and q_s are both functions of time due to the transient nature of the phase change process, and are also both functions of x due to effect of fluid flow and boundary layer growth in the x direction. For example, it is expected that q_s will be greatest at small x where convective heat transfer due to fluid flow is the greatest. Similarly, it is expected that q_s will reduce over time as the phase change front grows and slows down the rate of further phase change. Note that T_s and q_s are not known in advance, and must be determined by solving the governing equations presented above.

It is helpful to non-dimensionalize the set of equations here to ensure generality of the results. The following non-dimensionalization scheme is followed: $\theta_p = \frac{T_p - T_m}{T_\infty - T_m}$, $\theta_f = \frac{T_\infty - T_f}{T_\infty - T_m}$, $\xi = \frac{x}{L}$, $\eta = \frac{y}{L}$, $\tau = \frac{\alpha_p t}{L^2}$, $\bar{\alpha}_f = \frac{\alpha_f}{\alpha_p}$, $\bar{k}_f = \frac{k_f}{k_p}$, $\bar{u} = \frac{uL}{\alpha_p}$, $\bar{v} = \frac{vL}{\alpha_p}$, $\bar{\delta}_t = \frac{\delta_t}{L}$, $Ste = \frac{c_p(T_\infty - T_m)}{L_p}$. Note that L is an arbitrary length scale, which can be taken to be 1. $T_\infty - T_m > 0$ in the present melting problem. Based on this, the non-dimensional equations needed to be solved to determine the temperature field and propagation of the melting front can be expressed as follows: On the fluid side,

$$\frac{\partial \bar{u}}{\partial \xi} + \frac{\partial \bar{v}}{\partial \eta} = 0 \tag{13}$$

$$\bar{u}\frac{\partial \bar{u}}{\partial \xi} + \bar{v}\frac{\partial \bar{u}}{\partial \eta} = Pr \cdot \bar{\alpha}_f \frac{\partial^2 \bar{u}}{\partial \eta^2} \tag{14}$$

$$\bar{\alpha}_f \frac{\partial^2 \theta_f}{\partial \eta^2} = \frac{\partial \theta_f}{\partial \tau} + \bar{u}\frac{\partial \theta_f}{\partial \xi} + \bar{v}\frac{\partial \theta_f}{\partial \eta} \tag{15}$$

$$\theta_f = 0 \qquad at\ \eta \geq \bar{\delta}_t \tag{16}$$

$$\bar{u} = \bar{U}_\infty;\ \bar{v} = 0 \qquad at\ \eta \geq \bar{\delta} \tag{17}$$

$$\theta_f = 0; \bar{u} = \bar{U}_\infty \qquad at\ \xi = 0 \tag{18}$$

where $Pr = \nu_f/\alpha_f$ is the Prandtl number and $\bar{U}_\infty = U_\infty L/\alpha_p$ is the non-dimensional freestream velocity.

On the PCM side,

$$\frac{\partial^2 \theta_p}{\partial \eta^2} = \frac{\partial \theta_p}{\partial \tau} \tag{19}$$

$$\theta_p = 0 \qquad at\ \eta = \eta_{LS} \tag{20}$$

$$-Ste\frac{\partial \theta_p}{\partial \eta} = \frac{d\eta_{LS}}{d\tau} \qquad at\ \eta = \eta_{LS} \tag{21}$$

Where $\eta_{LS}(\tau) = y_{LS}/L$ is the non-dimensional location of the phase change front.

Finally, at the PCM-fluid interface,

$$\theta_f = \theta_s;\ \theta_p = 1 - \theta_s \qquad at\ \eta = 0 \tag{22}$$

$$\bar{k}_f \frac{\partial \theta_f}{\partial \eta} = -\frac{\partial \theta_p}{\partial \eta} = G(\xi, \tau) \qquad at\ \eta = 0 \tag{23}$$

Where $G(\xi,\tau) = \frac{q_s(x,t)L}{k_p(T_\infty - T_m)}$ and $\theta_s(\xi,\tau) = \frac{T_\infty - T_s(x,t)}{T_\infty - T_m}$ are the non-dimensional interface flux into the PCM and temperature distribution, respectively.

Eqs. (13)-(23) along with the initial condition ($\theta_p = 0;\ \theta_f = 0$ at $\tau = 0$) fully define the conjugate heat transfer problem considered here. Section 2.4 discusses an iterative approach to solve this problem by dividing it into two sub-problems and utilizing temperature and heat flux conservation at the interface to match the two solutions. This technique utilizes solutions for two sub-problems in the PCM and flow regions, respectively, which are first presented in the next two sub-sections.

2.2. Solution of Phase Change Sub-Problem

The problem defined in section 2.1 is solved iteratively, making use of two previously reported techniques to solve the PCM and fluid flow problems separately [9,26]. Figs. 2(a) and 2(b) show schematics of the two separate sub-problems. Solutions of the two sub-problems are needed to drive the iterative procedure. Solution for the PCM and fluid flow sub-problems are described in this and next sub-section, respectively. The iterative technique that combines these two solutions is discussed in section 2.4.

First, the PCM problem is considered. In this case, the governing equations are given by equations (19)-(21). Boundary condition at the PCM-flow interface, $\eta = 0$ is taken to be given by Eq. (23). Since heat transfer within the PCM in x direction is neglected, therefore, for any location x, this is a problem of one-dimensional phase change with time-dependent heat flux boundary condition. A perturbation method based solution of this problem has been presented in the literature [9]. Assuming that Ste is small, the perturbation method expresses the temperature distribution in a power series involving Ste. By using the energy balance at the phase change front as well as the time-dependent heat flux boundary condition specified at $\eta = 0$, the following expression is derived for the temperature distribution at any location ξ [9]:

$$\theta_p = \theta_0(\eta, \eta_{LS}) + Ste \cdot \theta_1(\eta, \eta_{LS}) + Ste^2 \cdot \theta_2(\eta, \eta_{LS}) \tag{24}$$

where

$$\theta_0(\eta, \eta_{LS}) = -G(\eta - \eta_{LS}) \tag{25}$$

$$\theta_1(\eta, \eta_{LS}) = G\left[-\frac{G'}{\eta'_{LS}}\left(\frac{\eta^3 - \eta_{LS}^3}{6}\right) + \left(G + \frac{G'}{\eta'_{LS}}\eta_{LS}\right)\left(\frac{\eta^2 - \eta_{LS}^2}{2}\right)\right] \tag{26}$$

$$\theta_2(\eta, \eta_{LS}) = \frac{A}{20}\left(\eta^5 - \eta_{LS}^5\right) + \frac{B}{12}\left(\eta^4 - \eta_{LS}^4\right) + \frac{C}{6}\left(\eta^3 - \eta_{LS}^3\right) + \frac{D}{2}\left(\eta^2 - \eta_{LS}^2\right) \tag{27}$$

$$A = -\frac{1}{6}G\left(\left[\frac{G'}{\eta'_{LS}}\right]^2 + \frac{G''}{\left(\eta'_{LS}\right)^2}G\right) \tag{28}$$

$$B = \frac{1}{2}G\left(\eta_{LS}\left(\left[\frac{G'}{\eta'_{LS}}\right]^2 + \frac{G''}{\left(\eta'_{LS}\right)^2}G\right) + 3G\frac{G'}{\eta'_{LS}}\right) \tag{29}$$

$$C = G\frac{G'}{\eta'_{LS}}\left[\eta_{LS}\left(\eta_{LS}\frac{G'}{\eta'_{LS}} + G\right) - \frac{G'}{\eta'_{LS}}\frac{\eta_{LS}^2}{2}\right] \tag{30}$$

$$D = \left[\begin{array}{l} -G\left(\eta_{LS}\frac{G'}{\eta'_{LS}} + G\right)\left(\eta_{LS}\left(\eta_{LS}\frac{G'}{\eta'_{LS}} + G\right) - \frac{G'}{\eta'_{LS}}\frac{\eta_{LS}^2}{2}\right) + \\ G\left(-2G\frac{G'}{\eta'_{LS}}\eta_{LS}^2 - \eta_{LS}G^2 - \frac{1}{3}\eta_{LS}^3\left(\left[\frac{G'}{\eta'_{LS}}\right]^2 + \frac{G''}{\left(\eta'_{LS}\right)^2}G\right)\right) \end{array}\right] \tag{31}$$

where $'$ and $''$ refer to differentiation with respect to time.

In equations (25)-(31), the location of the phase change front is given by solving the following differential equation [9]

$$\frac{d\eta_{LS}}{d\tau} = -Ste\left[\begin{array}{c} -G + Ste \times G\left(\left(y_{LS}\frac{G'}{y'_{LS}} + G\right)y_{LS} - \frac{G'}{y'_{LS}}\frac{y_{LS}^2}{2}\right) + \\ Ste^2\left(\frac{A}{4}y_{LS}^4 + \frac{B}{3}y_{LS}^3 + \frac{C}{2}y_{LS}^2 + Dy_{LS}\right) \end{array}\right] \quad (32)$$

with an initial condition of $\eta_{LS} = 0$ at the initial time.

As discussed in section 2.4, the temperature at the PCM-fluid interface obtained from Eq. (24) is used for convection heat transfer analysis of the fluid flow sub-problem, which is discussed next.

2.3. Solution of Convective Heat Transfer Sub-Problem

The fluid flow sub-problem is defined by equations (13)-(18), along with the boundary condition given by Eq. (22), which describes a time-dependent and space-dependent temperature $\theta_s(\xi,\tau)$ at $\eta = 0$. The fluid flow sub-problem, therefore, is the problem of convective heat transfer to/from a hydrodynamically developed laminar flow with a time-dependent and space-dependent base temperature. The interest is in solving this problem to determine the interface heat flux as a function of space and time, $G(\xi,\tau)$. While standard solutions are available for this problem for the special case of a constant plate temperature [20], the case of a temperature that varies in both space and time – as is the case for the PCM melting problem being discussed here – is more complicated. Recently, a solution for this problem has been proposed through the use of Karman-Pohlhausen polynomials [26]. In this technique, the velocity and temperature distributions within the fluid flow are expressed in terms of third-order Karman-Pohlhausen polynomials. Coefficients of these polynomials are chosen to satisfy all boundary conditions, which is known to result in very good accuracy [20]. By inserting these expressions in the energy conservation Eq. (15), the following partial differential equation can be derived [26]:

$$r^3 + 4\xi r^2\frac{\partial r}{\partial \xi} + 2\xi r^3\frac{1}{\theta_s}\frac{\partial \theta_s}{\partial \xi} + 5\frac{\xi}{\bar{U}_\infty}\left[\frac{r^2}{\theta_s}\frac{\partial \theta_s}{\partial \tau} + r\frac{\partial r}{\partial \tau}\right] = \frac{13}{14}Pr \quad (33)$$

Where $r = \frac{\bar{\delta}_t}{\bar{\delta}}$ and $\bar{\delta} = 4.64\sqrt{\frac{\bar{\alpha}_f Pr\xi}{\bar{U}_\infty}}$. Further,

$$r = 0 \qquad at\ \tau = 0 \quad (34)$$

$$r = 0 \qquad at\ \xi = 0 \quad (35)$$

Once Eq. (33) is solved, heat flux at the plate interface is determined by

$$G(\xi,\tau) = \frac{3}{2}\frac{\bar{k}_f\theta_s(\xi,\tau)}{\left[4.64\sqrt{\frac{\bar{\alpha}_f Pr\xi}{\bar{U}_\infty}}\right]r(\xi,\tau)} \quad (36)$$

The interface temperature $\theta_s(\xi,\tau)$ appearing in Eq. (33) is known from the plate boundary condition. While an analytical solution of Eq. (33) is unlikely to exist, a numerical integration of Eq. (33) can be carried out easily [26]. As discussed in the next sub-section, the heat flux determined in this manner, given by Eq. (36) is used in the iterative approach to solve the combined, conjugate heat transfer problem.

2.4. Iterative Technique

An iterative technique is used to combine the solutions of the two sub-problems described in sections 2.2 and 2.3 in order to solve the combined problem. Fig. 3 shows a flowchart of this iterative process for solving the conjugate problem involving both PCM and fluid flow regions. This technique starts by assuming a distribution for the interfacial heat flux, $G(\xi,\tau)$. Based on this, the PCM sub-problem is solved, as described in section 2.2. Specifically, the interfacial temperature distribution $\theta_s(\xi,\tau) = 1 - \theta_p(\xi,\eta = 0,\tau)$ is determined using Eq. (24). $\theta_s(\xi,\tau)$ is then used to solve the flow sub-problem as described in section 2.3. The interfacial flux distribution $G(\xi,\tau)$ computed from the solution of the flow sub-problem, given by Eq. (36) is computed. This is used to update the assumed interfacial heat flux distribution. A blend factor β ($0<\beta \leq 1$) is used to combine the old and computed flux distributions to provide the new flux distribution, with which to carry out the next iteration. Convergence is obtained when the interfacial flux and temperature distributions do not change significantly from one iteration to the other.

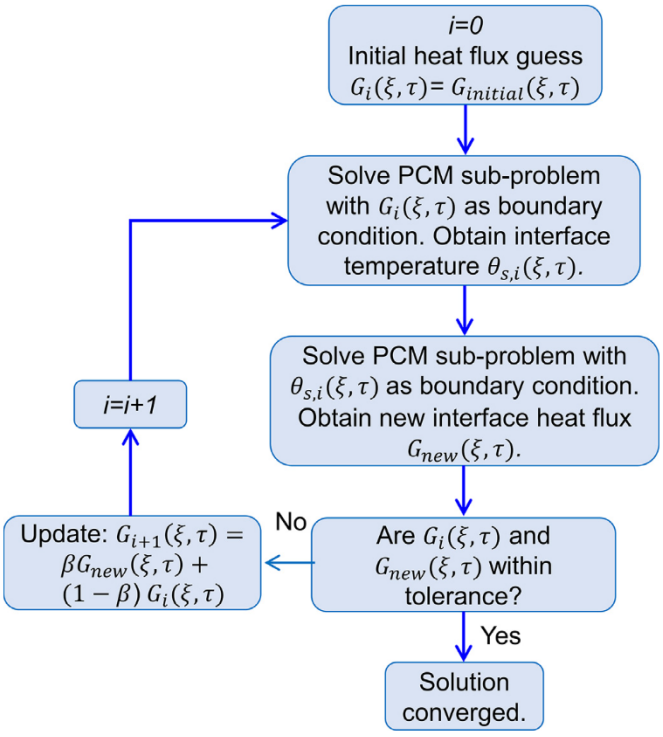

Fig. 3. Flowchart of the iterative approach used for solving the conjugate PCM-flow problem, based on solutions of the individual PCM and flow sub-problems.

3. Results and Discussion

The iterative technique for solving the conjugate PCM-flow problem discussed in section 2 is first compared with numerical computation results. Comparison is first carried out for the two sub-problems individually, followed by comparison for the complete conjugate problem.

For the PCM sub-problem, as shown in Fig. 2(a), heat flux on the surface of the PCM bed is specified, $G = G_0(1 - \frac{\xi}{\xi_0})exp(1 - \frac{\tau}{\tau_0})$, with $G_0 = 3333.34$, $\xi_0 = 0.15$, $\tau_0 = 8.36 \times 10^{-5}$. Since there is no fluid flow considered for the validation of the PCM sub-problem alone, therefore a value of $T_\infty - T_m = 1K$ is used for non-dimensionalization. For this case, propagation of the phase change front with time, $\eta_{LS}(\tau)$, based on Eq. (32) is compared with a finite-difference based numerical simulation code. This code solves the phase change propagation problem by dividing the domain into equally spaced spatial nodes, and determines the time taken for the phase change front to grow from one node to the next [27]. The accuracy of the simulation code is verified separately by comparison with the well-known solutions for a one-dimensional Stefan problem with constant temperature or constant heat flux boundary conditions [19]. This comparison is presented in Fig. 4(a) at three different locations, ξ, on the PCM bed. Results show excellent agreement between the present model and past work at

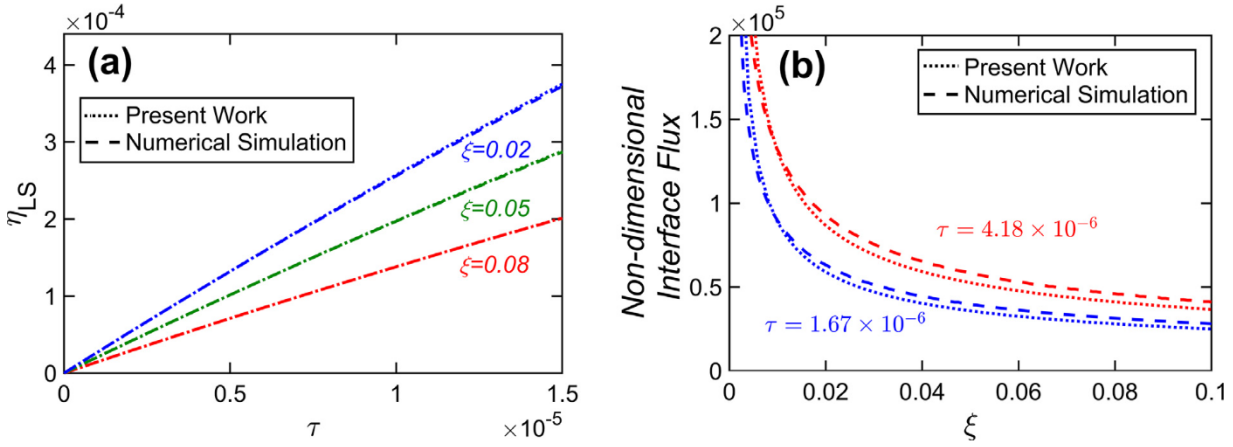

Fig. 4. Validation of solutions of individual sub-problems: (a) PCM sub-model: Comparison of model predictions with numerical simulation in terms of η_{LS} vs τ at three different locations for a given surface flux $G = G_0(1 - \frac{\xi}{0.15})\exp(-\frac{\tau}{\tau_0})$, where $G_0 = 3333.34, \tau_0 = 8.36 \times 10^{-5}$. (b) Flow sub-model: Comparison of model predictions with numerical simulations in terms of predicted surface flux distribution at two different times for a given interface temperature $\theta_s = 5\sqrt{\xi} + 691.75\sqrt{\tau} + 20$.

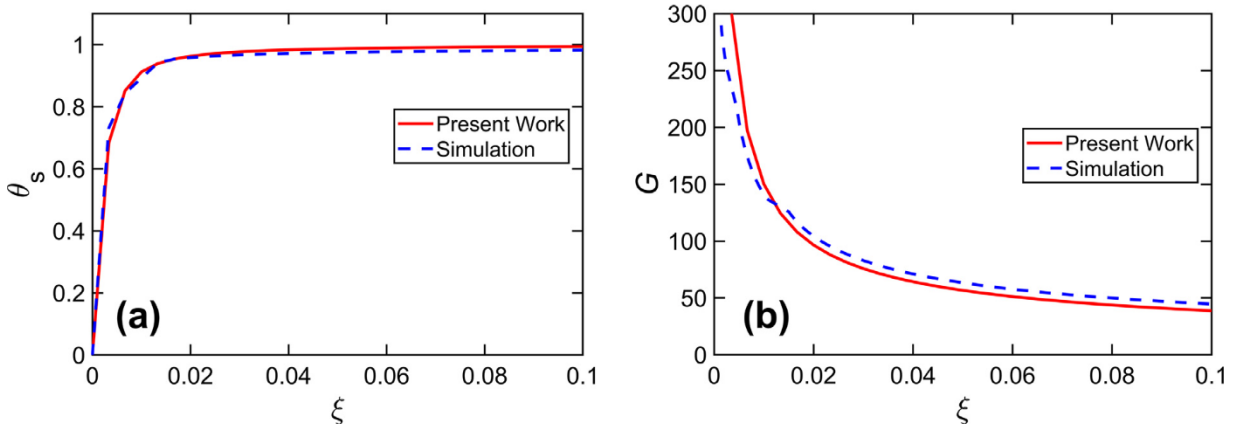

Fig. 5. Validation of iterative solution of the combined conjugate problem: (a) Surface temperature distribution, $\theta_s(\xi, \tau)$, and (b) Surface heat flux, $G(\xi, \tau)$ at $\tau = 8.36 \times 10^{-6}$. Plots from the present work are presented along with numerical simulation results. Problem parameters are $\bar{U}_\infty = 8.36 \times 10^8$, $Ste = 0.47$; $\bar{k}_f = 0.17$; $\bar{\alpha}_f = 250.56$ corresponding to octadecane PCM and room temperature air flow at 1 m/s freestream velocity.

each location and over the entire time duration considered. As expected, the phase change front grows with time at each location, and is the largest close to the leading edge (ξ=0.02), where convective heat transfer is most impactful. Comparison for the fluid flow sub-problem is presented in Fig. 4(b). For this comparison, a plate surface temperature of $\theta_s = 5\sqrt{\xi} + 691.75\sqrt{\tau} + 20$ is assumed as a representative temperature distribution at the PCM-flow interface. Based on this, interfacial heat flux is computed. Comparison of the results, with a finite-volume simulation code is presented in Fig. 4(b) for two different times. Validation of this simulation code has been carried out separately by comparison with analytical solutions for special cases [26]. There is good agreement between the two at both times. As expected, heat flux in response to the imposed temperature boundary condition is largest at small x, and decreases as x increases due to boundary layer growth. Heat flux also increases with time due to the nature of the imposed temperature boundary condition.

Further, a comparison of the solution of the complete conjugate problem with numerical simulations in a well-established finite-volume computational software is presented in Fig. 5. In this case, $\bar{U}_\infty = 8.36 \times 10^8$, $Ste = 0.47$, $\bar{k}_f = 0.17$, $\bar{\alpha}_f = 250.56$ corresponding to octadecane PCM and room temperature air flow at 1 m/s freestream velocity and at 50 °C above the melting temperature. Figs. 5(a) and 5(b) plot interface temperature and flux distribution along the bed at a fixed time, $\tau = 8.36 \times 10^{-6}$. Both Figures show excellent agreement between the present work and numerical simulations. As expected, the interface temperature grows from $\theta_s = 0$ at small ξ to $\theta_s = 1$ at large ξ. The interface flux reduces, sharply at first, and then gradually as ξ increases. Good agreement between the present work and numerical simulations – both for individual sub-problem and the combined conjugate problem – provides confidence about the accuracy of the model approach in the present work.

Due to the iterative nature of the conjugate technique presented in this work, it is important to also characterize iterative convergence and determine the number of iterations needed for a desired level of accuracy. While a general convergence analysis for this problem is mathematically cumbersome and difficult, the evolution of the computed solution over several iterations is investigated for a representative problem. For the same parameters as Fig. 5, except $Ste = 0.19$ corresponding to an imposed temperature difference of 20 °C, the computed temperature distribution at the PCM-flow interface at $\tau = 8.36 \times 10^{-6}$ is plotted at the end of one, three and five iterations in Fig. 6(a) with an initial guess of heat flux distribution of $G = 333.33$. The initial temperature distribution is also shown. Fig. 6(a) shows rapid convergence of the computed temperature distribution, which, stabilizes and does not show any appreciable change subsequent to three iterations. This indicates that for a typical PCM-flow problem, only around three iterations may be sufficient to reach a converged result. This finding is of

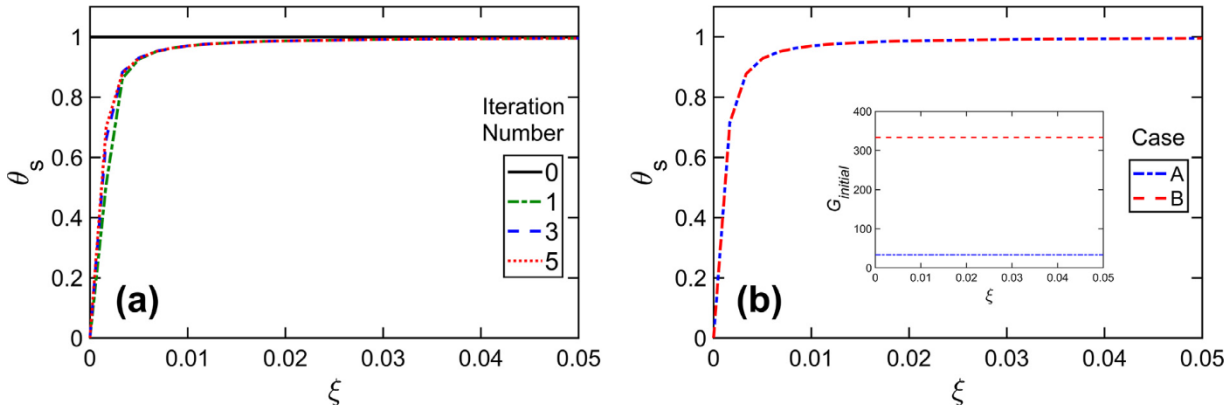

Fig. 6. Effect of number of iterations: (a) Predicted interface temperature distribution at $\tau = 8.36 \times 10^{-6}$ at the end of different number of iterations; (b) Converged interface temperature distribution at $\tau = 8.36 \times 10^{-6}$ for two different initial guesses of the interface heat flux, shown in inset. Problem parameters are $\bar{U}_\infty = 8.36 \times 10^8$, $Ste = 0.19$; $\bar{k}_f = 0.17$; $\bar{\alpha}_f = 250.56$ corresponding to octadecane PCM and room temperature air flow at 1 m/s freestream velocity.

much practical relevance, since a small number of iterations results in significant saving in computational cost.

In general, it is also important to determine the impact of the initial guess on the converged results and to verify that the converged solution is independent of the initial guess. This is particularly important when an initial guess may be significantly different from the converged solution. In order to investigate this, the iterative technique is carried out with two different initial guesses. The convergence of these two cases is shown in Fig. 6(b), in terms of temperature distributions at the end of three iterations, by when there is negligible change in the temperature distribution. It is seen that while the two cases considered here start from different points, both rapidly converge to the same temperature distribution. The temperature distributions at the end of three iterations for both cases are practically identical, as shown in Fig. 6(b).

Note that the iterative technique described in section 2 may be implemented with an initial guess of either the interface flux or temperature distribution. If guessing the interface temperature, it is helpful to first solve the flow problem, resulting in the interface flux that can be used to solve the PCM problem. A prediction of the interface temperature from the solution of the PCM problem can then be used to update the initial guess of the temperature distribution. A minor advantage of this approach compared to initial guess of heat flux is that the interface temperature is clearly bounded between 0 and 1, and therefore, an initial guess of 0.5 may be universally reasonable. On the other hand, bounds on the interface flux are not readily apparent.

3.1. Model Applications

The application of the iterative technique for understanding conjugate PCM-flow problems and the impact of various problem parameters on system performance is discussed next. The two key performance parameters of interest include the rate of phase change propagation into the PCM, and the amount of thermal energy entering the PCM. Fig. 7(a) plots distribution of the phase change front η_{LS} over the PCM bed at multiple times for a representative problem with $\bar{U}_\infty = 8.36 \times 10^8$, $Ste = 0.47$, $\bar{k}_f = 0.17$, $\bar{\alpha}_f = 250.56$ corresponding to octadecane PCM and room temperature air flow at 1 m/s freestream velocity and a freestream temperature of 50 °C above melting temperature. For the same problem, except with $Ste = 0.19$, Fig. 7(b) plots the heat flux into the PCM as a function of time at three different locations. As expected, the highest amount of phase change occurs close to the leading edge where the boundary layer is thinnest, resulting in very large rate of heat flow. As ξ increases, the boundary layer grows, heat flux reduces, and therefore, the extent of phase change is also lower. Further, Fig. 7(b) shows that the interfacial heat flux is very high at

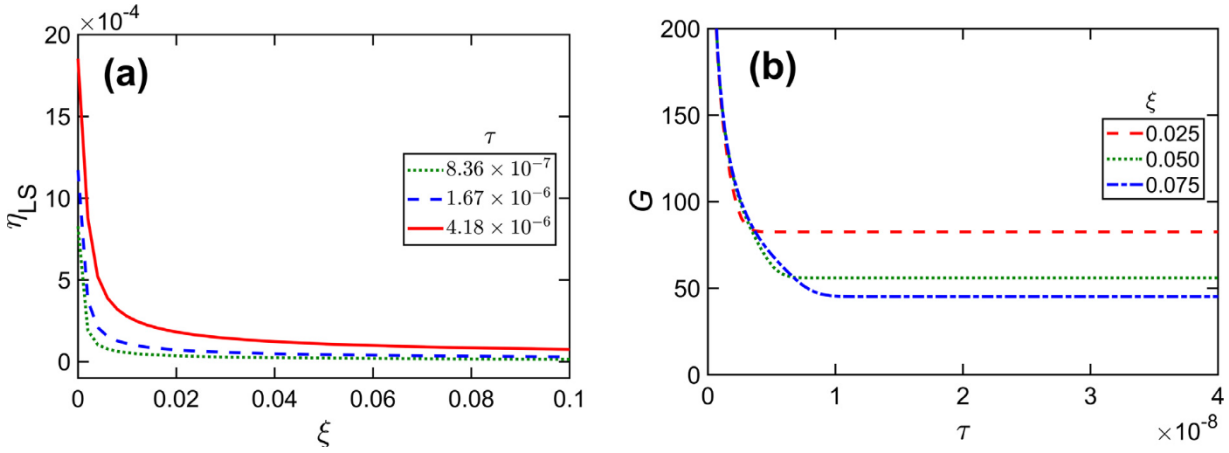

Fig. 7. Results from a representative PCM-flow conjugate problem: (a) Phase change propagation front η_{LS} vs ξ at three different times; (b) interfacial flux into the PCM as a function of τ at three different locations. Problem parameters are $\bar{U}_\infty = 8.36 \times 10^8$, $\bar{k}_f = 0.17$; $\bar{\alpha}_f = 250.56$ corresponding to octadecane PCM and room temperature air flow at 1 m/s freestream velocity. *Ste* is 0.47 and 0.19 in (a) and (b), respectively.

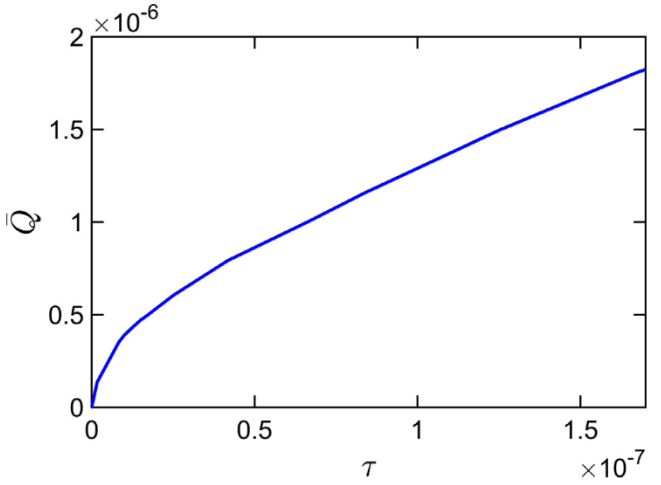

Fig. 8. Total energy stored in the PCM as a function of time for the problem parameters of Fig. 7(a).

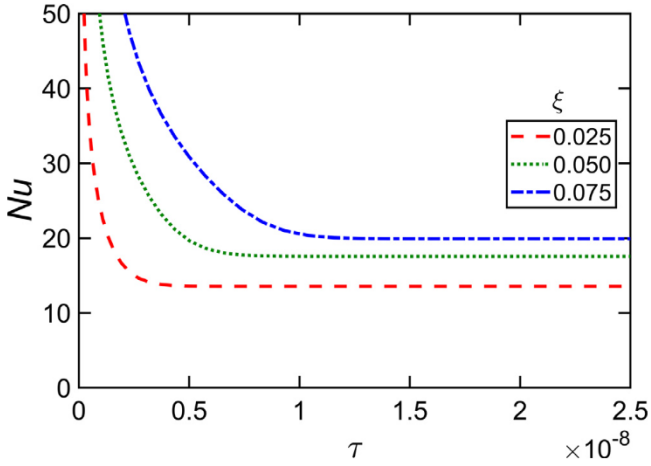

Fig. 9. Interfacial Nusselt number as function of time at three different locations for a representative PCM-flow conjugate problem. Problem parameters are $\bar{U}_\infty = 8.36 \times 10^8$, $Ste = 0.19$; $\tilde{k}_f = 0.17$; $\tilde{\alpha}_f = 250.56$ corresponding to octadecane PCM and room temperature air flow at 1 m/s freestream velocity.

initial times, and then rapidly decreases and saturates with time. The eventual interfacial heat flux is highest at small values of ξ, which is attributable to the effect of boundary layer growth.

Fig. 8 plots the total energy stored in the PCM as a function of time for the same set of parameters as Fig. 7(a). This quantity is obtained by integrating the heat flux at the PCM-flow interface over the length of the PCM bed which is 0.1 m and over time. As expected, Fig. 8 shows that the total energy stored in the PCM increases rapidly at first, when thermal resistance between freestream flow and phase change front is small. As the thicknesses of the boundary layer and melted PCM grow, the rates of phase change propagation and energy storage reduce, which is observed in Fig. 8. Note that the total energy stored in the PCM is the sum of latent heat stored due to phase change and sensible heat stored due to temperature rise in the melted PCM.

The convective heat transfer coefficient between the fluid flow and PCM, represented non-dimensionally by the Nusselt number is commonly used to represent the extent of convective heat transfer between the two. The transient nature of this problem, both due to boundary layer growth in the fluid flow as well as phase change propagation in the PCM implies that the convective heat transfer coefficient is not constant, but rather is a function of both space and time. While past work on PCM-fluid conjugate modeling relied on assuming a form of the Nusselt number [15,16], it is important to instead determine the Nusselt number from the solution of this problem. Based on the iterative technique discussed here, the variation in Nusselt number as a function of space and time is presented in Fig. 9. For the same set of parameters as the previous problem, except $Ste = 0.19$, Fig. 9 plots the Nusselt number as a function of time at three different locations. Fig. 9 shows, consistent with expectations, very high Nusselt number initially, which then decays rapidly over time and reaches a constant value at large time. At any time, the Nusselt number is highest at small ξ. Note that the Nusselt number is interpreted as the non-dimensional ratio of interfacial heat flux and temperature, neither of which are known or specified in advance.

The two key parameters on the fluid flow side that impact phase change and energy storage are the freestream velocity and freestream temperature. The impact of these parameters on the rate of phase change propagation in the PCM is investigated in Fig. 10. Fig. 10(a) plots η_{LS} distribution over the PCM bed at $\tau = 4.18 \times 10^{-6}$ for three different freestream velocities. A similar plot for three different freestream temperatures, represented by the Stefan number is presented in Fig. 10(b). An increase in either $\bar{U}_\infty$ or Ste results in greater convective heat transfer to the PCM

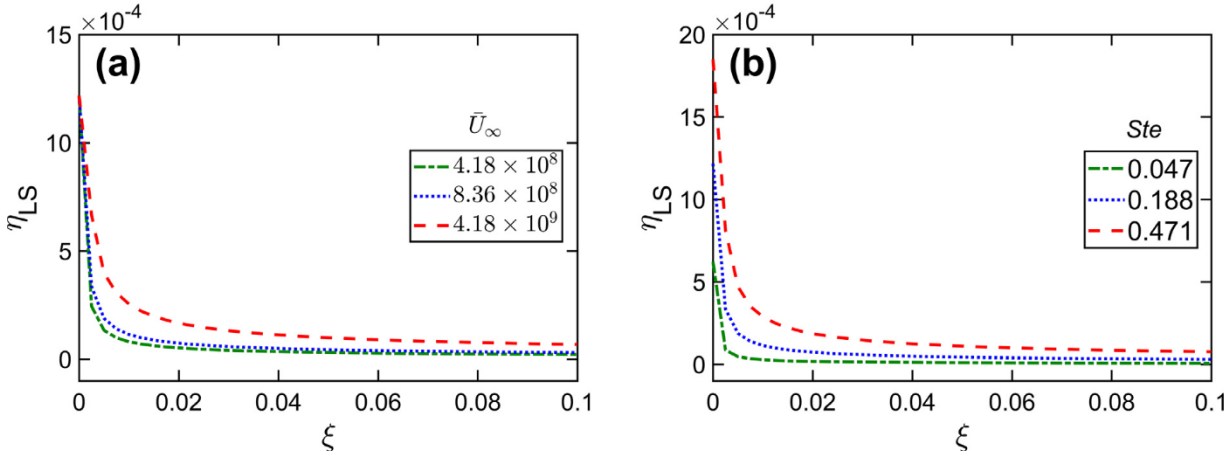

Fig. 10. Effect of key fluid flow parameters on phase change propagation: (a) η_{LS} vs ξ at $\tau = 4.18 \times 10^{-6}$ for three different values of $\bar{U}_\infty$, with $Ste = 0.19$; (b) η_{LS} vs ξ at $\tau = 4.18 \times 10^{-6}$ for three different values of Ste, with $\bar{U}_\infty = 8.36 \times 10^8$. Other problem parameters are $\tilde{k}_f = 0.17$; $\tilde{\alpha}_f = 250.56$ corresponding to octadecane PCM and room temperature air flow.

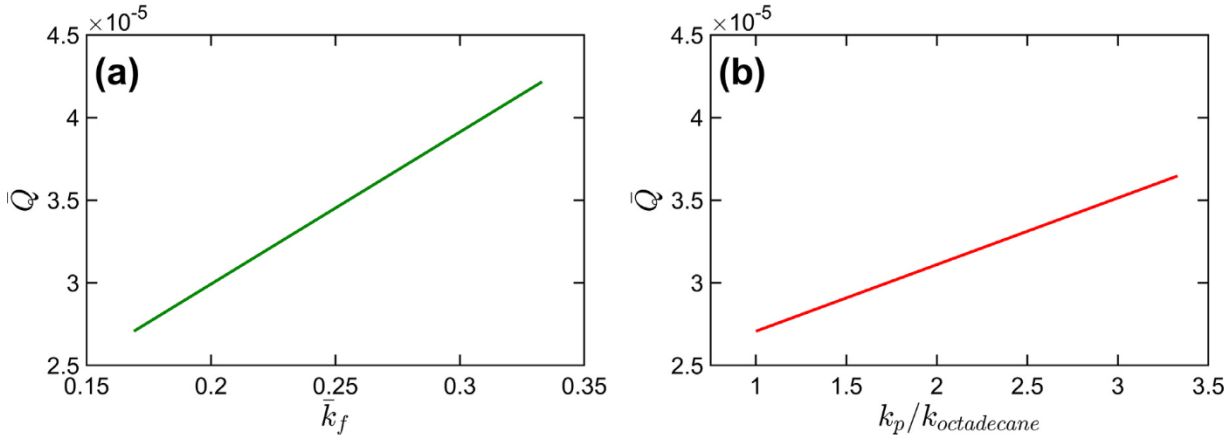

Fig. 11. Effect of key material properties on phase change propagation: Total energy stored in the PCM up to $\tau = 4.18 \times 10^{-6}$ as a function of thermal conductivity of (a) fluid and (b) PCM. Other problem parameters are $\bar{U}_\infty = 8.36 \times 10^8$, $Ste = 0.47$. Note that x axis in Figure (b) is non-dimensionalized on the basis of thermal conductivity of octadecane.

bed, and therefore, greater propagation of the phase change front into the PCM, as is clearly seen in these Figures. The impact of freestream velocity and temperature is particularly significant close to the leading edge (small ξ) where convective heat transfer is the greatest, whereas, at large ξ, Figs. 10(a) and 10(b) show diminished impact due to boundary layer growth and reduced convective heat transfer.

Thermal conductivities of the fluid and PCM are the key thermal properties that influence phase change propagation and energy storage. The impact of these properties on system performance is investigated next. Fig. 11(a) plots the total energy stored in the PCM as a function of thermal conductivity of the fluid, while holding all other parameters constant, including thermal conductivity of the PCM. A similar plot showing the total energy stored in the PCM as a function of thermal conductivity of PCM is plotted in Fig. 11(b), while other parameters, including thermal conductivity of the fluid are held constant. These plots show that the total energy stored is a much stronger function of thermal conductivity of the fluid than that of the PCM. For example, Figs. 11(a) and 11(b) show a much larger increase in energy stored when the fluid thermal conductivity is doubled, compared to doubling the PCM thermal conductivity. This indicates that under these conditions, the rate-limiting step in heat transfer and energy storage is on the fluid flow side rather than the PCM side. Therefore, for the present set of non-dimensional parameters, efforts towards improving energy storage must focus on improving convective heat transfer to/from the fluid rather than phase change heat transfer in the PCM. This may be an important insight into the design and optimization of practical energy storage systems.

4. Conclusions

Developing a robust theoretical understanding of heat transfer and phase change in flat bed latent energy storage systems is critical for design and optimization of practical systems. This work contributes in this direction by developing an iterative technique to obtain a closed-form solution for the temperature distribution, and hence, the rate of energy stored, in this system. The robustness of the iterative technique is established by comparison with numerical simulations, and by showing invariance of the computed solution with respect to the initial guess. The non-dimensional nature of analysis presented here helps generalize the results and ensure applicability to a range of PCMs and fluids. While presented in the context of a Cartesian system, the technique can be easily extended to cylindrical latent energy storage systems that are also encountered commonly. Further, the results can also be easily extended to problems involving a two-dimensional plate, although this would likely involve significant increase in computational cost.

It is important to recognize the key assumptions and limitations of the theoretical technique presented here. The convective heat transfer analysis assumes laminar, incompressible fluid flow. On the PCM side, key assumptions include small Stefan number and one-dimensional phase change propagation. All thermal properties are assumed to be constant. These are reasonable assumptions for a wide variety of applications.

The analytical technique developed in the present work may offer improved computational time and better insights into the fundamental nature of the heat transfer problem compared to numerical simulations. Further, analytical solutions may be easier to implement in realistic conditions than simulations, which may need specialized software to run. In addition to improving the theoretical understanding of heat transfer in a latent energy storage system, this work may also contribute towards design and optimization of practical engineering systems.

Declaration of Competing Interest

All authors hereby declare that they do not have conflicts of interest as described by Elsevier's policies (http://www.elsevier.com/conflictsofinterest).

CRediT authorship contribution statement

Amirhossein Mostafavi: Methodology, Investigation, Visualization, Data curation, Writing – original draft, Writing – review & editing. **Ankur Jain:** Conceptualization, Methodology, Supervision, Project administration, Writing – original draft, Writing – review & editing.

Acknowledgments

This material is based upon work supported by CAREER Award No. CBET-1554183 from the National Science Foundation. The authors would also like to gratefully acknowledge useful discussions with Dr. Mohammad Parhizi.

References

[1] I. Dincer, M. Rosen, Thermal energy storage: systems and applications, John Wiley & Sons, 2002.
[2] A. Bar-Cohen (Ed.), Encyclopedia of Thermal Packaging, Set 3: Thermal Packaging Applications, World Scientific Press, 2018.

[3] M. Parhizi, A. Jain, Analytical modeling and optimization of phase change thermal management of a Li-ion battery pack, Applied Thermal Engineering 148 (2019) 229–237.
[4] A. Mills, M. Farid, J.R. Selman, S Al-Hallaj, Thermal conductivity enhancement of phase change materials using a graphite matrix, Applied Thermal Engineering 26 (2006) 1652–1661.
[5] P. Lamberg, K. Siren, Approximate analytical model for solidification in a finite PCM storage with internal fins, Applied Mathematical Modelling 27 (7) (2003) 491–513.
[6] A. Mostafavi, M. Parhizi, A. Jain, Theoretical modeling and optimization of fin-based enhancement of heat transfer into a phase change material, International Journal of Heat and Mass Transfer 145 (2019) 118698.
[7] T. Rozenfeld, Y. Kozak, R. Hayat, G. Ziskind, Close-contact melting in a horizontal cylindrical enclosure with longitudinal plate fins: demonstration, modeling and application to thermal storage, International Journal of Heat and Mass Transfer 86 (2015) 465–477.
[8] J. Caldwell, Y.Y. Kwan, On the perturbation method for the Stefan problem with time-dependent boundary conditions, International Journal of Heat and Mass Transfer 46 (8) (2003) 1497–1501.
[9] M. Parhizi, A. Jain, Solution of the phase change Stefan problem with time-dependent heat flux using perturbation method, Journal of Heat Transfer 141 (2) (2019) 024503.
[10] M. Parhizi, A. Jain, The impact of thermal properties on performance of phase change based energy storage systems, Applied Thermal Engineering 162 (2019) 114154.
[11] V. Dubovsky, G. Ziskind, R. Letan, Analytical model of a PCM-air heat exchanger, Applied Thermal Engineering 31 (16) (2011) 3453–3462.
[12] M. Ezra, Y. Kozak, V. Dubovsky, G. Ziskind, Analysis and optimization of melting temperature span for a multiple-PCM latent heat thermal energy storage unit, Applied Thermal Engineering 93 (2016) 315–329.
[13] R.E. Murray, D. Groulx, Experimental study of the phase change and energy characteristics inside a cylindrical latent heat energy storage system: Part 1 consecutive charging and discharging, Renewable Energy 62 (2014) 571–581.
[14] S.M. Vakilaltojjar, W. Saman, Analysis and modelling of a phase change storage system for air conditioning applications, Applied Thermal Engineering 21 (3) (2001) 249–263.
[15] C. Ding, Z. Niu, B. Li, D. Hong, Z. Zhang, M. Yu, Analytical modeling and thermal performance analysis of a flat plate latent heat storage unit, Applied Thermal Engineering 179 (2020) 115722.
[16] M. Bechiri, K. Mansouri, Exact solution of thermal energy storage system using PCM flat slabs configuration, Energy Conversion and Management 76 (2013) 588–598.
[17] M. Lacroix, Study of the heat transfer behavior of a latent heat thermal energy storage unit with a finned tube, International Journal of Heat and Mass Transfer 36 (8) (1993) 2083–2092.
[18] D. Arnold, Dynamic simulation of encapsulated ice stores. Part I: the model, ASHRAE Trans 97 (2) (1990) 1170–1178.
[19] V. Alexiades, A.D. Solomon, Mathematical modeling of melting and freezing processes, Routledge, 2018.
[20] W.M. Kays, M.E. Crawford, B. Weigand, Convective heat and mass transfer, McGraw-Hill Higher Education, Boston, 2005.
[21] A.S. Dorfman, Conjugate problems in convective heat transfer, CRC Press, 2009.
[22] K. Shah, A. Jain, An iterative, analytical method for solving conjugate heat transfer problems, International Journal of Heat and Mass Transfer 90 (2015) 1232–1240.
[23] D. Chalise, K. Shah, R. Prasher, A. Jain, Conjugate heat transfer analysis of thermal management of a Li-ion battery pack, Journal of Electrochemical Energy Conversion and Storage 15 (1) (2018) 011008.
[24] M. Parhizi, A. Jain, Analytical modeling and optimization of phase change thermal management of a Li-ion battery pack, Applied Thermal Engineering 148 (2019) 229–237.
[25] M. Parhizi, M. Pathak, J.K. Ostanek, A. Jain, An iterative analytical model for aging analysis of Li-ion cells, Journal of Power Sources (2021) In press, doi:10.1016/j.jpowsour.2021.230667.
[26] A. Mostafavi, A. Jain, Theoretical analysis of unsteady convective heat transfer from a flat plate with time-varying and spatially-varying temperature distribution, International Journal of Heat and Mass Transfer 183 (2022) 122061 in review, doi:10.1016/j.ijheatmasstransfer.2021.122061.
[27] D.W. Hahn, M.N. Özişik, Heat Conduction, Wiley, New York, 2012.